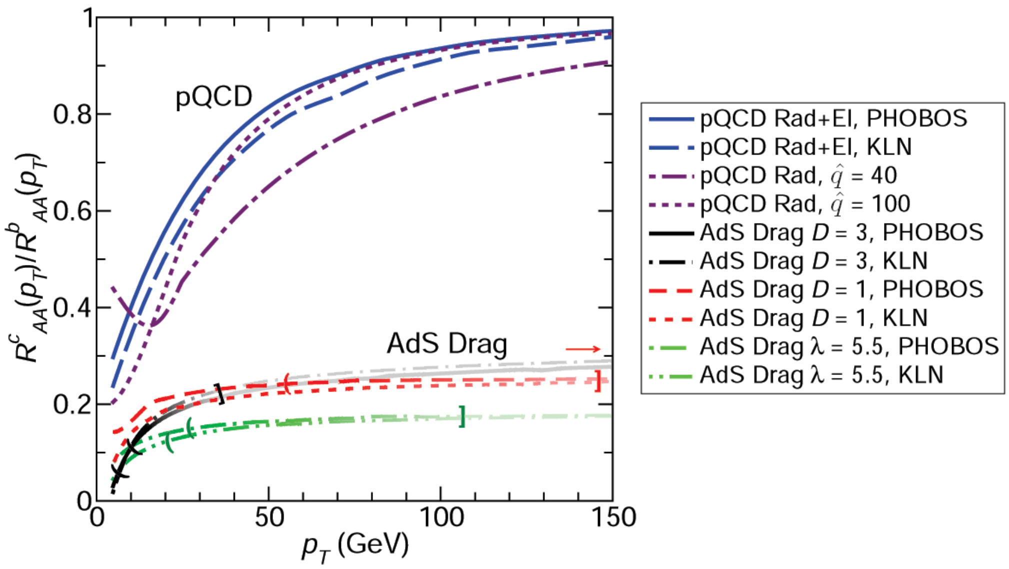

Figure 5.3: *The double ratio of $R^c_{AA}(p_T)$ to $R^b_{AA}(p_T)$ predictions for* Lhc *using Eq. (5.1) for AdS/CFT and WHDG [152] for pQCD with a wide range of input parameters. The generic difference between the pQCD results tending to unity contrasted to the much smaller and nearly p_T-independent results from AdS/CFT can be easily distinguished at* Lhc*. The "(" and "]" denote momenta after which possible string theoretic corrections may need to be considered; the curves' increasing transparency from "(" to "]" is meant to additionally emphasize this, see text.*

$\kappa L^2 \hat{q} \log(p_T/M_Q)/p_T$, with κ a proportionality constant and $\hat{q} = \mu_D^2/\lambda_g$. The most important feature in pQCD relative to AdS/CFT is that $\bar{\epsilon}_{pQCD} \to 0$ asymptotically at high-p_T while $\bar{\epsilon}_{AdS}$ remains constant. $n_Q(p_T)$ is a slowly increasing function of momentum, Fig. 5.4; thus R^{pQCD}_{AA} increases with p_T whereas R^{AdS}_{AA} decreases. This generic difference can be observed in Fig. 5.2, which shows representative predictions from the full numerical calculations of